Original paper

Can the histological type of colorectal cancer determine the carcinogenesis pathway?

Małgorzata Kołos, Anna Wasążnik-Jędras, Anna Nasierowska-Guttmejer

Department of Pathomorphology in Warsaw, Central Clinical Hospital of the Ministry of the Interior, Warsaw, Poland

Colorectal cancer (CRC) is the most common type of gastrointestinal cancer and has three major pathways of carcinogenesis. About 80% of genomic instability concerns chromosomal instability (CIN); the rest is connected with either microsatellite instability (MSI) or CpG island methylation. Some MSI-related cancers are associated with Lynch syndrome, whereas others are caused by sporadic, acquired hypermethylation of the promoter of the MLH1 gene. These tumours have distinctive clinical and histopathological features. They may be poorly differentiated, accompanied by Crohn's-like lymphocytic infiltration and have a pushing margin. MSI-high (MSI-H) phenotype has a slightly better prognosis. We investigated 46 classic CRCs using histochemical and immunohistochemical methods (p53, MLH1, MSH2, MSH6). Based on the results, we divided patients into 4 groups. Tumours from the first and second group (27 cases) expressed the loss of MSI markers and presented a characteristic clinical and morphological image. The other 19 cases lacked significant immunohistochemical or microscopic features. These require further molecular studies to evaluate their carcinogenesis. Discovery of MSI in colorectal tumours should be taken into account in the management of patients. They do not respond to 5-fluorouracil or anti-EGFR therapy, especially the sporadic ones with BRAF mutations.

Key words: colorectal cancer, microsatellite instability (MSI), hypermethylation of the promoter of the MLH1 gene, MSI-H phenotype, BRAF.

Introduction

Colorectal cancer (CRC) is an epithelial cancer originating from the colon or from the rectum. Data from the Polish National Cancer Registry from 2012 show that CRC is the second most common cancer among women and the third most common cancer among men in Poland [1]. Most CRC cases are classic adenocarcinomas, while others are either undifferentiated, neuroendocrine or squamous cell cancers. Colorectal cancer usually appears among patients older than 60. These neoplasms are mostly sporadic cancers preceded by precancerous states. Among younger people CRC is mostly of hereditary origin. The heterogeneity of colorectal cancer is a result of the presence of three different carcinogenesis pathways which correlate with the clinical and morphological manifestation [2, 3]. We distinguish cancers with chromosomal instability (CIN), microsatellite instability (MSI) and cancers with CpG island methylator phenotype (CIMP) [4-6].

Chromosomal instability remains the origin for the vast majority of CRC (80% of cases), mostly associated with sporadic cancers caused by gene accumulation in the somatic cells and with a low percentage (1%) of hereditary cancers such as familial adenomatous polyposis (FAP) or the MUTYH polyposis syndrome [7]. These cancers develop as a result of *APC*, *KRAS*, *TP53* or *MUTYH* gene mutation. The phenotype of these tumours is associated with the classic pathway

of transformation from adenoma to adenocarcinoma described by Fearon and Vogelstein in 1990 [8].

Microsatellite instability is present in about 15% of colorectal cancers. Most of them (12%) are sporadic cancers with epigenetic disorders in the MLH1 hypermethylation promoter which results in the occurrence of the MSI-H type of CRC [9]. Only 3% of CRC are associated with the mutation pathway, in which a mutation appears in the mismatch repair (MMR) DNA genes of the germinal cells [10]. This results in the Lynch syndrome, first described as hereditary non-polyposis colorectal cancer (HNPCC) [11]. The carcinogenesis in the sequence from adenoma to adenocarcinoma remains similar to the CIN pathway. However, cancers caused by MSI are characterised by better prognosis, a distinct microscopic view and a different response to chemotherapy [12]. The diagnostic algorithm includes clinical features listed in the Bethesda Guidelines and the Amsterdam Criteria, as well as the microscopic characteristics of MSI-H (high) cancers, such as older age of patients, right-sided location, medullary and mucinous cancer type, and Crohn's-like inflammatory infiltrate presence.

The third pathway of carcinogenesis is associated with the hypermethylation of CpG islands (CIMP), which is preceded by serrated polyps. In these cases *BRAF* gene mutation can also occur [13, 14].

State-of-the-art methods in modern pathology include immunohistochemical assays to determine MSI as an important prognostic and predictive factor for patient survival and therapy.

Aim

The aim of this study was to isolate MSI-H colorectal cancers on the basis of their microscopic imaging and immunohistochemical tests among typical colorectal adenocarcinomas.

Material and methods

The study material consisted of 46 specimens of colorectal cancer (including one case of bifocal cancer) from 45 patients treated from 2007 to 2013 in the Central Clinical Hospital of the Ministry of Interior in Warsaw. The majority of the analysed data come from the 2009-2010 period.

One of the specimens came from an oligobiopsy of a tumour taken during an endoscopic procedure. The rest of the material was collected after surgery (right-sided or left-sided hemicolectomy, sigmoidectomy or proctectomy). One of the patients with rectal cancer was given neoadjuvant radiotherapy prior to the operation. In order to analyse the clinico-pathological data, we divided the study material into two groups: the first consists of specimens obtained after right-sided surgery, which includes the caecum, the ascending colon and the transverse colon; the second group consists of left-sided tumours from the descending colon, the sigmoid and the rectum.

The tissue material was fixed in 10% buffered formalin. The tissue samples from post-operative specimens and the tumour material from the oligobiopsy were embedded in paraffin. The sections of 4 μm thickness were stained with haematoxylin and eosin (HE). We examined the histological type and the tumour grade based on the WHO classification [blue book] [15] and the tumour stage based upon the 7th edition of AJCC/UICC pTNM (*American Joint Committee on Cancer/Union internationale contre le cancer*) [16]. Microscopic features characteristic for MSI-H cancers[17] were also analysed including the presence and type of inflammatory infiltrate (diffuse or Crohn's-like), tissue heterogeneity including mucus and signet ring cell presence, necrosis in the tumour stroma and the type of tumour growth pattern (spreading or penetrating).

Protein expression products of mutator genes MLH1, MSH2, MSH6 and TP53 protein accumulation was examined by immunohistochemical assays. Immunohistochemical tests were prepared by the fully automated Ventana BenchMark GX instrument, and the following antibodies were used: MLH1 (anti-MLH1 M1 Mouse Monoclonal Primary Antibody 5 ml (~1.4 μg/ml), Ventana), MSH2 (MSH2 219-1129 Mouse Monoclonal Antibody 2.27 μg/ml, Cell Marque), MSH6 (CONFIRM anti-MSH6 44 Mouse Monoclonal Primary Antibody 5 ml (~0.101 μg/ml), Ventana) and TP53 (Anti-p53 Bp53-11 Primary Antibody 5 ml (~2.5 μg/ml).

To analyse the immunohistochemical reaction the following criteria were applied:

1) For the mutator gene MLH1, MSH2, MSH6 proteins:
   - *lack of nuclear staining* as proof of microsatellite instability (MSI), diagnosed in cases of loss of immunohistochemical expression of MLH1, MSH2 and MSH6 proteins,
   - *nuclear staining* as proof of microsatellite stability (MSS) found in cases with the immunohistochemical nuclear expression of MLH1, MSH2 and MSH6 proteins.

In all cases, internal positive and negative controls were performed. The positive control was IHC nuclear expression of the analysed proteins in lymphocytes. The internal negative control was a specimen of an adenocarcinoma without loss of expression (MSS).

2) For accumulation of the TP53 protein:
   - a positive reaction was asserted in cases of IHC nuclear expression of 100% of cells or a focal nuclear reaction from 10% to 30% of cells ("restricted p53 overexpression"),
   - a negative reaction was diagnosed in case of loss of expression in more than 90% of cell nuclei [18].

Results

Clinical data: 46 cases of colorectal cancer were analysed, coming from 45 patients. More than half of tumours came from female patients – 25 cases (54%). The mean age was 66.5 years in the case of females and 70.3 among males. The youngest patient was 29 years old, and the oldest was 90 years old.

Right-sided cancers were diagnosed in 27 cases (59%), while left-sided cancers were diagnosed in 19 cases (41%). The most common locations were the caecum in 12 cases (26%) and the sigmoid in 10 cases (21%). The right-sided location was dominant among female patients, observed in 19 out of 27 cases (70%). Among male patients most of the cases were left-sided – 13 cases out of 19 (68%). Clinical data and macroscopic features of colorectal cancer are presented in Table I.

Macroscopically: Exophytic tumours constituted 23 cases (50%), endophytic 19 (41%) and mesophytic (intramural) 4 (9%). The smallest diameter of a tumour was 1.5 cm and the biggest was 13 cm. The mean size was 4.2 cm (standard deviation 2.27 cm) both for the left-sided and right-sided location. Clinical data and macroscopic features are presented in Table I.

Microscopically: Classic adenocarcinomas were diagnosed in 87% of cases, both in the left-sided and right-sided location. Two cases of medullary carcinomas and one case of mucinous carcinoma were diagnosed among female patients in the caecum. The second case of mucinous carcinoma was diagnosed in a male patient and it was located on the left side. Moreover, in the male patient group there was a case of neuroendocrine cancer, being the second cancer focus along with the adenocarcinoma (2%). One case of mixed adenoneuroendocrine carcinoma (MANEC) (2%) was also present in this group. In both locations most of the cancers were locally advanced (pT3 or pT4) G2 neoplasms – 36 cases (78%). Microscopic features of left- and right-sided adenocarcinomas are presented in Table II.

Right-sided tumours more often presented tissue heterogeneity, signet ring cells, produced mucus and had a spreading growth pattern. They also more commonly presented chronic inflammatory infiltrates of diffuse and mixed type (diffuse type and Crohn's-like) compared to the left-sided tumours. Necrosis was equally common in both locations. Microscopic features of tumours are presented in Tables III and IV.

Immunohistochemical (IHC) assays: IHC loss of expression of mutator gene proteins (loss of nuclear

Table I. Clinical data and macroscopic features of colorectal cancers

Location, sex, exact anatomic location	Number of cases	Mean tumour size	Mean age
Left-sided	**19**	**4.3**	**65.7**
Females	6	3.1	61.5
Sigmoid	4	2.8	61.0
Rectum	2	3.8	62.5
Males	13	4.8	67.7
Sigmoid	6	5.0	70.3
Rectum	2	5.3	67.0
Ascending colon	2	3.3	58.0
Descending colon	3	5.2	69.3
Right-sided	**27**	**4.2**	**69.9**
Females	19	4.5	67.9
Caecum	9	5.1	70.0
Transverse colon	4	4.5	68.5
Ascending colon	6	3.7	64.5
Males	8	3.3	74.5
Caecum	3	3.0	79.0
Transverse colon	2	2.0	64.5
Ascending colon	3	4.0	76.7
Total	**46**	**4.2**	**68.2**

Table II. Histological type, grading and staging of the tumours and their right- and left-sided location

Location	Histological type	Tumour grade	TNM	Number of cases
Left side	Adenocarcinoma	G1	pT3N0	2
		G2	pT1Nx	1
			pT3N0	3
			pT3N1a	2
			pT3N1b	2
			pT3N1c	1
			pT3N2a	2
			pT3N2b	1
			pT3N2bM1	1
		GX	pT2N1b	1
	Mucinous adenocarcinoma	G3	pT1N0	1
	Neuroendocrine carcinoma	G3	pT4N0	1
	MANEC	G3	pT3N2bM1	1
Right side	Adenocarcinoma	G1	pT2N0	1
		G2	no data	1
			pT1N0	1
			pT2N0	4
			pT3N0	4
			pT3N1a	5
			pT3N1b	1
			pT3N2aM1	1
			pT3N2b	1
			pT3N2bM1a	1
			pT3N2bM1b	1
			pT4aN0	1
			pTm3N1b	1
		G3	pT3N2a	1
	Mucinous adenocarcinoma	G2	pT2N0	1
	Medullary carcinoma	G4	pT3aN2a	1
			pT3N2a	1
Total				46

staining) was found in 12 out of 46 cases. The IHC loss of expression of MLH1 was observed in 9 cases, all of which were right-sided and with MSH2 and MSH6 expression (nuclear staining present). The loss of expression of MSH2 (along with loss of MSH6) only appeared in 2 left-sided cases. In 37 cases there was no loss of MLH1 expression, in 31 tumours there was a strong nuclear staining reaction, and in 6 cases it was classified as heterogeneous and weak. In only one case (a right-sided tumour) MSH2 expression was classified as weak in nuclei of single cells. The immunostaining for MSH6 was mostly heterogeneous in both distribution and intensity.

No TP53 protein accumulation was found in 17 cases, 9 of them right-sided. Positive reaction for TP53 occurred in 29 cases. In 19 of those cases the staining was very strong and diffuse in the whole sample (10 right-sided and 9 left-sided cases). The re-

Table III. Histological type and microscopic features of the tumours. No data concern the specimen after oligobiopsy. Mucus presence means under 50% of tumour tissue

Location	Anatomical location	Histological type	Tumour grade	TNM	Inflammatory infiltrate	Mucus	Signet ring cells	Necrosis	Tissue heterogeneity	Tumour growth pattern
L	Sigmoid	Adenocarcinoma	G1	pT3N0	Absent	Absent	Absent	Absent	Absent	Penetrating
L	Sigmoid	Adenocarcinoma	G1	pT3N0	Present, diffuse	Absent	Absent	Absent	Absent	Spreading with budding
L	Sigmoid	Adenocarcinoma	G2	pT3N1a	Present, diffuse	Absent	Absent	Present	Absent	Penetrating
L	Sigmoid	Adenocarcinoma	G2	pT3N0	Present, diffuse	Present	Absent	Present	Present	Penetrating
L	Sigmoid	Adenocarcinoma	G2	pT3N1c	Absent	Present	Absent	Present	Present	Penetrating
L	Sigmoid	Adenocarcinoma	G2	pT3N2bM1	Absent	Absent	Absent	Present	Absent	Spreading with budding
L	Sigmoid	Adenocarcinoma	G2	pT3N2a	Absent	Absent	Absent	Present	Present	Spreading
L	Sigmoid	Adenocarcinoma	G2	pT1Nx	Absent	Absent	Absent	Absent	Absent	Penetrating
L	Sigmoid	Adenocarcinoma	G2	pT3N2b	Absent	Absent	Absent	Present	Absent	Penetrating
L	Sigmoid	Adenocarcinoma	G2	pT3N1b	Present, diffuse	Absent	Absent	Present	Present	Penetrating
L	Rectum	Adenocarcinoma	G2	pT3N1b	Present, diffuse +Crohn's-like	Present	Absent	Present	Absent	Spreading
L	Rectum	Adenocarcinoma	G2	pT3N0	Present, diffuse	Absent	Absent	Present	Present	Penetrating
L	Rectum	Adenocarcinoma	G2	pT3N1a	Absent	Absent	Absent	Present	Present	Spreading
L	Rectum	Adenocarcinoma	GX	ypT2N1b	Present, diffuse	Absent	Absent	Present	Absent	Penetrating
L	Ascending colon	Mucinous adenocarcinoma	G3	pT1N0	Absent	Present	Absent	Absent	Present	Penetrating
L	Ascending colon	Neuroendocrine carcinoma	G3	pT4N0	Present, diffuse	Absent	Absent	Absent	Absent	Penetrating
L	Descending colon	Adenocarcinoma	G2	pT3N0	Present, diffuse	Absent	Absent	Present	Absent	Spreading
L	Descending colon	Adenocarcinoma	G2	pT3N2a	Present, Crohn's-like	Present	Absent	Absent	Present	Penetrating
L	Descending colon	MANEC	G3	pT3N2bM1	Present, diffuse +Crohn's-like	Absent	Absent	Present	Present	Penetrating

Table III. Cont.

Location	Anatomical location	Histological type	Tumour grade	TNM	Inflammatory infiltrate	Mucus	Signet ring cells	Necrosis	Tissue heterogeneity	Tumour growth pattern
R	Caecum	Adenocarcinoma	G1	pT2N0	Absent	Absent	Absent	Absent	Absent	Spreading
R	Caecum	Adenocarcinoma	G2	pT3N1a	Present, diffuse +Crohn's-like	Absent	Absent	Absent	Present	Spreading
R	Caecum	Adenocarcinoma	G2	pTm3N1b	Present, diffuse +Crohn's-like	Absent	Absent	Present	Present	Spreading
R	Caecum	Adenocarcinoma	G2	pT2N0	Present, diffuse +Crohn's-like	Present	Present	Absent	Present	Spreading
R	Caecum	Adenocarcinoma	G2	pT3N0	Present, diffuse	Present	Absent	Present	Present	Spreading
R	Caecum	Adenocarcinoma	G2	pT3N1a	Present, diffuse	Present	Absent	Absent	Present	Penetrating
R	Caecum	Adenocarcinoma	G2	pT4aN0	Present, diffuse	Absent	Absent	Present	Absent	Penetrating
R	Caecum	Adenocarcinoma	G2	pT3N1a	Present, diffuse	Present	Absent	Present	Present	Penetrating
R	Caecum	Adenocarcinoma	G2	pT-3N2bM1a	Present, diffuse	Absent	Absent	Absent	Absent	Penetrating
R	Caecum	Adenocarcinoma	G3	pT3N2a	Present, diffuse	Present	Present	Present	Present	Spreading
R	Caecum	Mucinous adenocarcinoma	G2	pT2N0	Present, diffuse +Crohn's-like	Present	Absent	Absent	Present	Spreading with budding
R	Caecum	Medullary carcinoma	G4	pT3N2a	Present, diffuse	Absent	Absent	Present	Present	Penetrating
R	Transverse colon	Adenocarcinoma	G2	No data	Present, diffuse	Present	Absent	Present	Present	No data
R	Transverse colon	Adenocarcinoma	G2	pT3N0	Present, diffuse	Absent	Absent	Absent	Absent	Penetrating
R	Transverse colon	Adenocarcinoma	G2	pT3N1a	Present, diffuse +Crohn's-like	Absent	Absent	Present	Absent	Penetrating
R	Transverse colon	Adenocarcinoma	G2	pT2N0	Present, diffuse	Present	Absent	Present	Present	Penetrating
R	Transverse colon	Adenocarcinoma	G2	pT3N0	Absent	Absent	Absent	Absent	Absent	Penetrating
R	Transverse colon	Medullary carcinoma	G4	pT3a-N2a	Present, diffuse	Absent	Absent	Present	Absent	Spreading
R	Ascending colon	Adenocarcinoma	G2	pT3N2b	Present, diffuse	Absent	Absent	Present	Absent	Penetrating
R	Ascending colon	Adenocarcinoma	G2	pT2N0	Present, diffuse +Crohn's-like	Present	Absent	Absent	Present	Penetrating

Table III. Cont.

Location	Anatomical location	Histological type	Tumour grade	TNM	Inflammatory infiltrate	Mucus	Signet ring cells	Necrosis	Tissue heterogeneity	Tumour growth pattern
R	Ascending colon	Adenocarcinoma	G2	pT2N0	Present, diffuse +Crohn's-like	Present	Absent	Present	Present	Spreading
R	Ascending colon	Adenocarcinoma	G2	pT3N1a	Present, diffuse	Absent	Absent	Present	Present	Penetrating
R	Ascending colon	Adenocarcinoma	G2	pT3N2aM1	Present, diffuse	Absent	Absent	Present	Present	Penetrating
R	Ascending colon	Adenocarcinoma	G2	pT1N0	Present, diffuse	Absent	Absent	Absent	Absent	Penetrating
R	Ascending colon	Adenocarcinoma	G2	pT3N1b	Present, diffuse	Absent	Absent	Absent	Present	Penetrating
R	Ascending colon	Adenocarcinoma	G2	pT3N0	Present, Crohn's-like	Absent	Absent	Absent	Present	Penetrating
R	Ascending colon	Adenocarcinoma	G2	pT3N2bM1b	Present, diffuse +Crohn's-like	Present	Absent	Present	Present	Penetrating

maining 10 tumours presented heterogeneous staining (2 left-sided cases and 8 right-sided). Detailed results of the immunohistochemical analysis depending on the location are presented in Table V.

Depending on the IHC assay results the cases were divided into four groups, which are presented in Table VI. The first group includes cancers characterised by loss of expression of at least one MSI-H marker, the second group contains tumours with TP53 protein accumulation, and the remaining two groups are composed of cases with negative or heterogeneous immunohistochemical assay results.

Discussion

The results of this study indicate that there exists a correlation between clinical data, microscopic features, immunohistochemical marker expression and the potential carcinogenesis pathway. The majority of the analysed cases are classic adenocarcinomas. Based on the microscopic imaging and IHC results, we can define the probable carcinogenesis pathway in tumours from the first and the second group (altogether 27 cases). Twelve cancers from the first group develop on the basis of microsomal instability, and 15 of the cancer cases from group 2 develop on the basis of chromosomal instability. In the remaining 19 tumours from groups

Table IV. Microscopic features divided into the left-sided and the right-sided location

Microscopic feature	L	R
Necrosis		
Present	13 (28.3%)	15 (32.6%)
Absent	6 (13%)	12 (26.1%)
Inflammatory infiltrate		
Diffuse	8 (17.4%)	16 (34.8%)
Crohn's-like	1 (2.2%)	1 (2.2%)
Diffuse + Crohn's-like	2 (4.3%)	8 (17.4%)
Absent	8 (17.4%)	2 (4.3%)
Mucus		
Present	5 (10.9%)	11 (23.9%)
Absent	14 (30.4%)	16 (34.8%)
Signet ring cells		
Present	(0%)	2 (4.3%)
Absent	19 (41.3%)	25 (54.3%)
Tissue heterogeneity		
Present	9 (19.6%)	18 (39.1%)
Absent	10 (21.7%)	9 (19.6%)
Margin		
Spreading	13 (28.3%)	17 (37%)
Penetrating	4 (8.7%)	8 (17.4%)
Penetrating with budding	2 (4.3%)	1 (2.2%)
No data	(0%)	1 (2.2%)

Table V. Immunohistochemical assay results. Loss of expression of tested markers – loss of staining (MSI carcinomas). Expression of markers (no loss of expression) – nuclear staining or weak staining (MSS)

Localisation	P53	MLH1	MSH2	MSH6	Number of cases
Left-sided	Positive	Expression	Expression	Expression	7
	Positive	Reduced expression	Expression	Expression	2
	Positive patches	Expression	Expression	Expression	1
	Positive patches	Expression	Loss of expression	Loss of expression	1
	Negative	Expression	Expression	Expression	5
	Negative	Expression	Expression	Loss of expression	1
	Negative	Expression	Loss of expression	Expression	1
	Negative	Reduced expression	Expression	Expression	1
Right-sided	Positive	Expression	Expression	Expression	7
	Positive	Reduced expression	Expression	Expression	2
	Positive	Reduced expression	Reduced expression	Expression	1
	Positive patches	Expression	Expression	Expression	1
	Positive patches	Loss of expression	Expression	Expression	7
	Negative	Expression	Expression	Expression	7
	Negative	Loss of expression	Expression	Expression	2
Total					46

Table VI. Cases divided into groups depending on the IHC assay results

Group	Number of cases	P53	MSI
1	12	Negative or heterogeneous	≥ 1 gene marker with loss of expression
2	15	Positive or heterogeneous	Expression
3	13	Negative	Expression
4	6	Positive or negative	Reduced expression of MLH1 or MSH2

3 and 4, determination of the exact mechanism of carcinogenesis requires additional molecular tests. The neoplastic transformation in those cases might be linked to the CIMP pathway. However, none of the tumours presented the serrated phenotype. The cases from the first group (26%) are characterised by the loss of expression of at least one of the following markers: *MLH1*, *MSH2*, *MSH6.* The IHC assays results show MSI linked to the Lynch syndrome or sporadic cancer with MLH1 promoter hypermethylation. In the second group (33% of cases) the tumours presented TP53 protein accumulation and expression of MSI markers, which may suggest a suppressor carcinogenesis pathway.

Figures 1-8 images present the microscopic view (HE) and IHC results.

Apart from the additional tests' results, the potential carcinogenesis pathway can be indicated by the tumour morphology (this applies to the cases from the first and the second group).

It is worth noting that most of the cases microscopically presented as classic adenocarcinomas – 7 cases (58%) in the first group and all cases (100%) in the second group.

Additionally, in group 1 there were 2 cases (17%) of mucinous carcinomas, 2 cases (17%) of medullary carcinomas and 1 (8%) neuroendocrine carcinoma (Fig. 9).

In the first group, the microscopic features of MSI-H were evidenced by Crohn's-like lymphocyte infiltrates (Figs.10, 11), the presence of mucus with signet ring cells in certain tumour stroma (Fig. 12) and a spreading growth pattern in most cases.

Only one of 12 cases in the second group (80%) had confirmed chronic lymphocytic inflammatory infiltrate. Similarly, only one case (6%) presented inflammatory Crohn's-like infiltrate (Fig. 13).

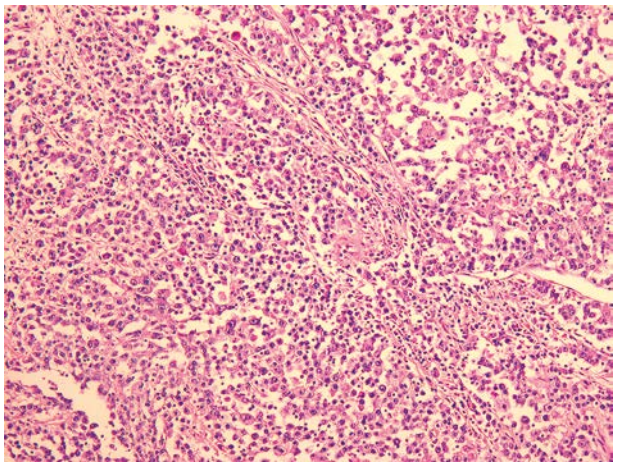

Fig. 1. Medullary carcinoma, HE, medium magnification

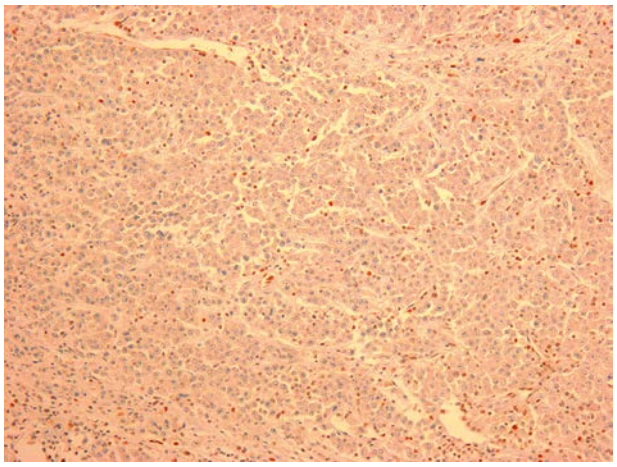

Fig. 2. Medullary carcinoma, loss of MLH1 expression (loss of nuclear staining), medium magnification

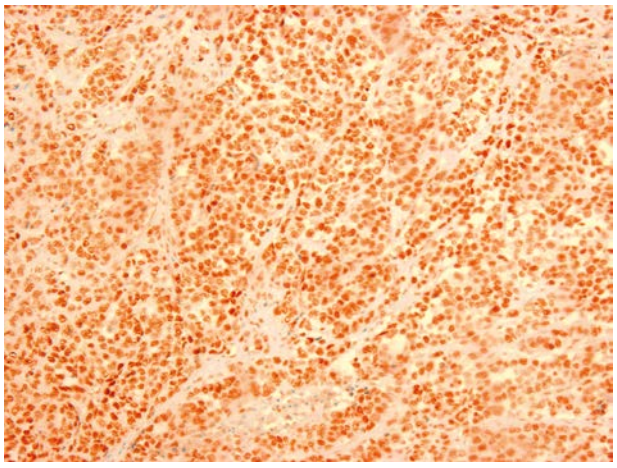

Fig. 3. Medullary carcinoma, MSH2 expression (no loss of expression), medium magnification

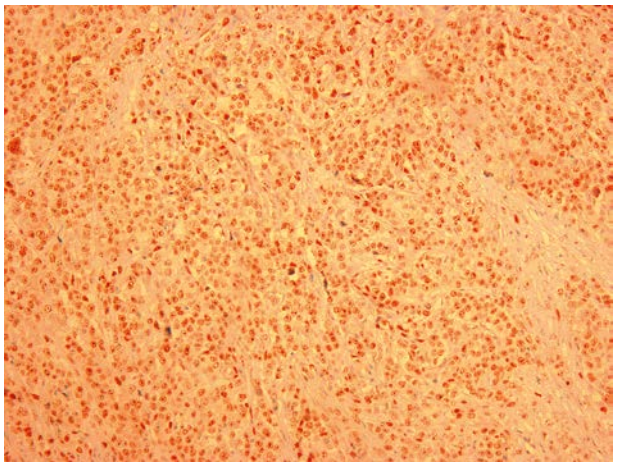

Fig. 4. Medullary carcinoma, MSH6 expression (heterogeneous reaction), medium magnification

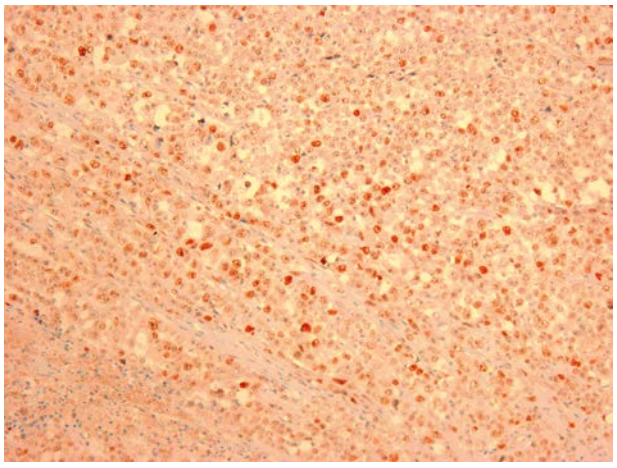

Fig. 5. Medullary carcinoma, TP53 patchy reaction, medium magnification

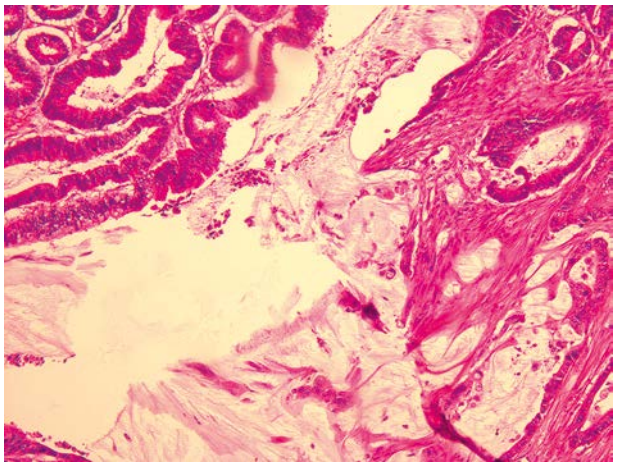

Fig. 6. Mucinous carcinoma, HE, medium magnification

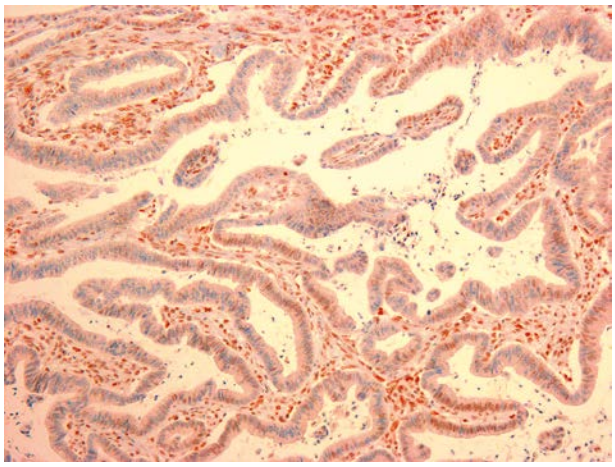

Fig. 7. Mucinous carcinoma, loss of MLH1 expression (loss of nuclear staining), medium magnification

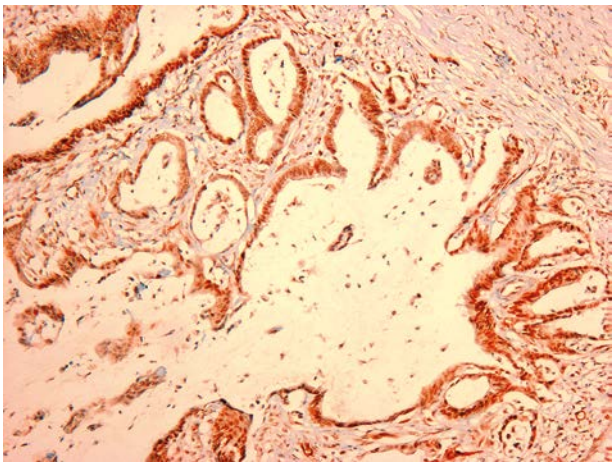

Fig. 8. Mucinous carcinoma, MSH2 expression (no loss of expression), medium magnification

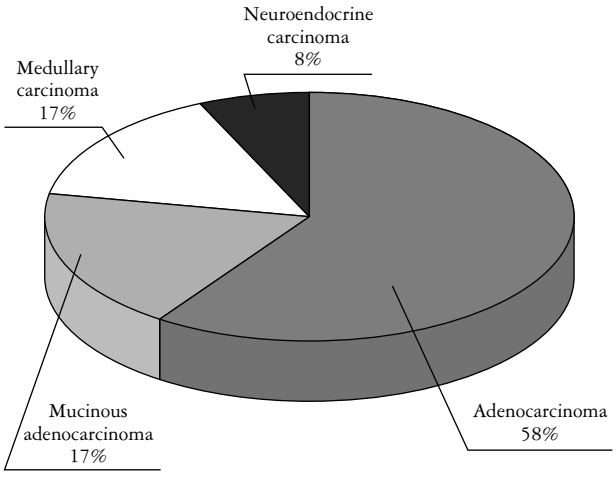

Fig. 9. Histological types of tumours in group 1 (left-sided)

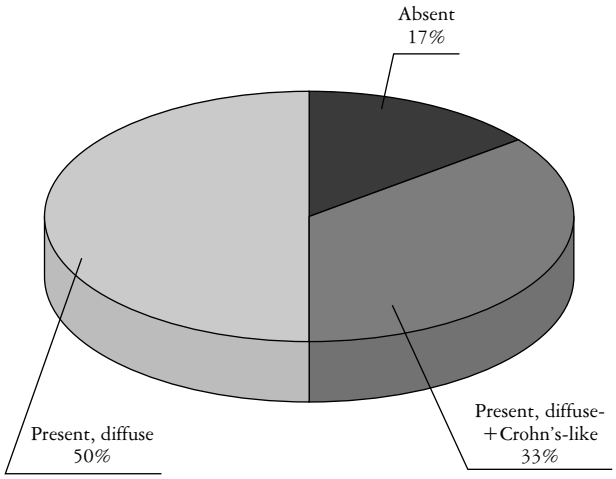

Fig. 10. Properties of inflammatory infiltrates in group 1 (right-sided)

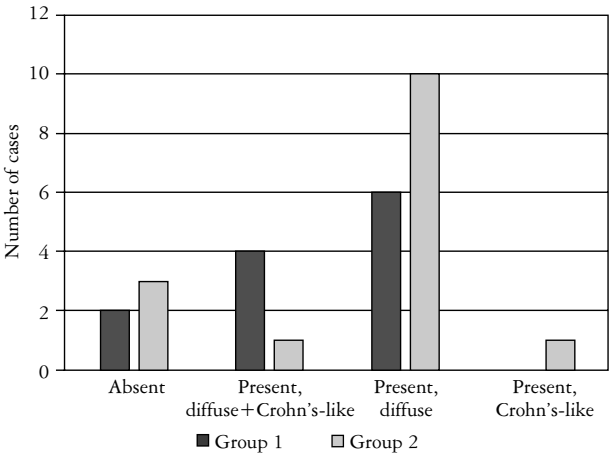

Fig. 11. Comparison of inflammatory infiltrates between groups 1 and 2

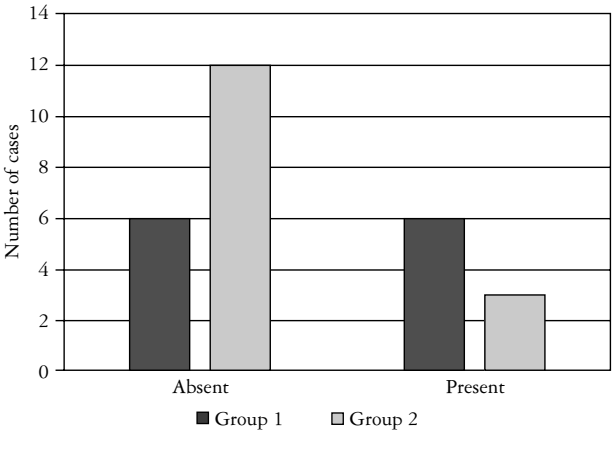

Fig. 12. Comparison of mucus presence in tumours between group 1 and 2 specimens

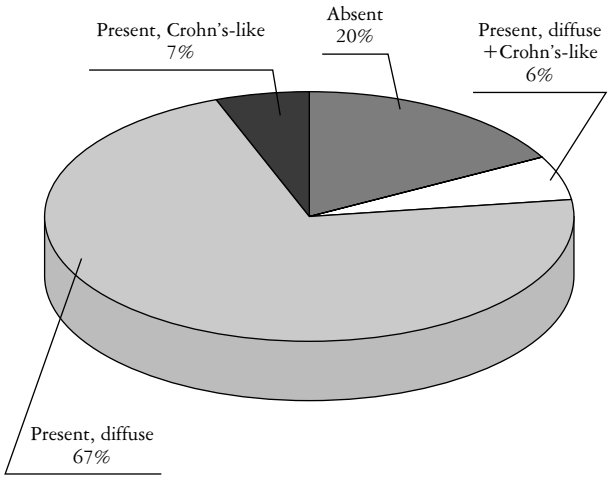

Fig. 13. Features of inflammatory infiltrates in group 2 (left-sided)

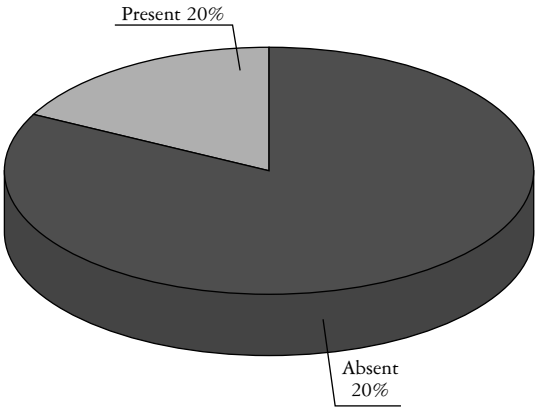

Fig. 14. Presence of mucus in tumours of the second group (right-sided)

Mucus was found among 3 carcinomas (20%) (Fig. 14). Most of the tumours were characterised by a penetrating growth pattern (93%).

In comparison to classic adenocarcinomas, cancers with MSI-H presented different clinical features (Fig. 15). Cancers from group 1 occurred more often on the right side in the caecum (58%), more commonly among older patients, especially female. In contrast, group 2 presented no such correlation in terms of patient gender or location. Nevertheless, among these patients metastases to the lymph nodes were more common (9 cases – 60%) compared to patients from group 1 (6 cases – 50%).

In all studied groups the predominant neoplasm was the classic adenocarcinoma. The microscopic analysis and IHC assay results permitted MSI-H cancers to be distinguished. Membership of a given group was not determined by the histological type of tumour. Colorectal cancers with microsatellite instability and presentation of the classic adenocarcinoma showed loss of expression of MLH1. Poorly differentiated adenocarcinomas and classic mucinous carcinomas, which both have bad prognosis, need to be distinguished from adenocarcinoma with MSI, presenting quite similarly under the microscope but having a better prognosis. The differential diagnosis should also include neuroendocrine carcinoma and lymphoma [19, 20]. In these cases the IHC assays should include the following tests: CK7, CK20, synaptophysin, chromogranin A and LCA.

It is important to highlight that one microscopic feature cannot determine the carcinogenesis pathway. Rare medullary carcinomas in which cells create syncytial cell formations accompanied by diffuse lymphocytic infiltrates around the tumour need to be differentiated from the classic, poorly differentiated adenocarcinomas without MSI-H [21] and characterised by a poorer prognosis. Conversely, cases with mucus lakes in the tumour stroma are often misdiagnosed as classic mucinous adenocarcinoma, while in fact being mucinous carcinoma with MSI features characterised by a better prognosis, indicated by cases in the first group of this study.

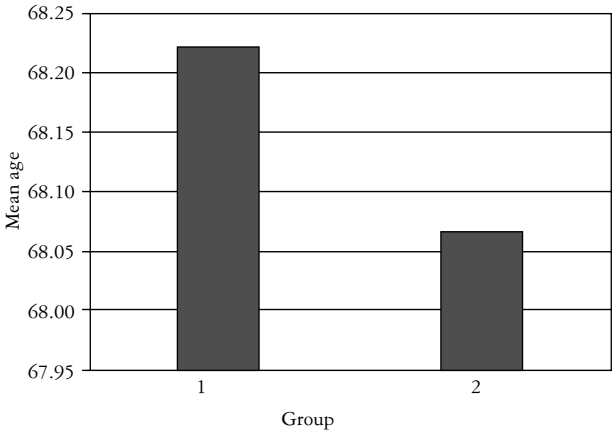

Fig. 15. Comparison of mean age of patients between groups 1 and 2

In order to differentiate cancers with MSI-H from classic colorectal adenocarcinomas, it is necessary to perform additional testing for microsatellite instability. A thorough analysis of clinical data including family history, patient's age and the location of the tumour with its microscopic features such as histological and inflammatory infiltrate type, tissue heterogeneity and the growth pattern can be helpful to distinguish MSI-H cancers. Recognition of those cases might be useful in the clinical scenario. Studies show that colorectal cancers with *MLH1* promoter hypermethylation (sporadic cancers) are effective prognostic and predictive factors [22]. They are associated with better prognosis and worse response to chemotherapy with 5-fluorouracil. There are ongoing studies analysing the better response of MSI-H cancers to irinotecan. The recognition of *MLH1* promoter hypermethylation additionally allows one to

recognize patients with *BRAF* gene mutation, which is diagnosed among 70% of patients with this type of cancer. It is associated with the lack of response to anti-EGFR therapy. *BRAF* gene mutation testing is indicated by the ASCO/CAP 2013 guidelines as an important prognostic and predictive factor among patients with MSI-H colorectal cancer.

The authors declare no conflict of interest.

References

1. Wojciechowska U, Didkowska J, Zatoński W. Nowotwory w Polsce w 2012 roku. Nowotwory 2013; 63: 197-216
2. Bosman FT. Colorectal cancer. In: World Cancer Report 2014. Stewart BW, Wild CP (eds.). IARC Press, Lyon 2014; 32-402.
3. Fearon ER Molecular genetics of colorectal cancer. Annu Rev Pathol Mech Dis 2011; 6: 479-507.
4. Budinska E, Popovici V, Tejpar S, et al. Gene expression patterns unveil a new level of molecular heterogeneity in colorectal cancer. J Pathol 2013; 231: 63-76.
5. Jass JR. Classification of colorectal cancer based on correlation of clinical, morphological and molecular features. Histopathology 2007; 50: 113-130.
6. Geurts-Giele WR, Leenen CH, Dubbink HJ .Somatic aberrations of mismatch repair genes as a cause of microsatellite-unstable cancers. J Pathol 2014; 234: 548-559.
7. Fearon ER, Vogelstein B. A genetic model for colorectal carcinogenesis. Cell 1996; 87: 159-170.
8. Fearon ER, Vogelstein B. A genetic model for colorectal tumorigenesis. Cell 1990; 61: 759-77.
9. Cunningham JM, Christensen ER, Tester DJ, et al. Hypermethylation of the hMLH1 promoter in colon cancer with microsatellite instability. Cancer Res 1998; 58: 3455-3460.
10. Nyström-Lahti M, Parsons R, Sistonen P, et al. Mismatch repair genes on chromosomes 2p and 3p account for a major share of hereditary nonpolyposis colorectal cancer families evaluable by linkage. Am J Hum Genet 1994; 55: 659-665.
11. Vasen HF, Watson P, Mecklin JP, et al. New clinical criteria for hereditary nonpolyposis colorectal cancer (HNPCC, Lynch syndrome) proposed by the International Collaborative group on HNPCC. Gastroenterology 1999; 116: 1453-1456.
12. Pino MS, Chung DC. Microsatellite instability in the management of colorectal cancer. Expert Rev Gastroenterol Hepatol 2011; 5: 385-399.
13. Issa JP. CpG island methylator phenotype in cancer. Nat Rev Cancer 2004; 4: 988-993.
14. Kambara T, Simms LA, Whitehall VL, et al. BRAF mutation is associated with DNA methylation in serrated polyps and cancers of the colorectum. Gut 2004; 53: 1137-1344.
15. WHO Classification of Tumours of the Digestive System. Bosman FT, Carneiro F, Hruban RH, Theise ND (eds.). IARC, Lyon 2010; 134-147.
16. TNM Classification of Malignant Tumors. International Union Against Cancer. Sobin LH, Gospodarowicz MK, Wittekind C (eds.). 7th ed. Wiley-Blackwell, Oxford 2009.
17. Nasierowska-Guttmejer A. Rak jelita grubego. W: Zalecenia do diagnostyki histopatologicznej nowotworów. Nasierowska-Guttmejer A, Górnicka B (red.). Wyd. Centrum Onkologii, Oddział Gliwice, Gliwice 2013; 99-106.
18. Nyiraneza C, Jouret-Mourin A, Kartheuser A, et al. Distinctive patterns of p53 protein expression and microsatellite instability in human colorectal cancer. Hum Pathol 2011; 42: 1897-1910.
19. Kazama Y, Watanabe T, Kanazawa et al. Microsatellite instability in poorly differentiated adenocarcinomas of the colon and rectum: relationship to clinicopathological features. J Clin Pathol 2007; 60: 701-704.
20. Imai Y. Poorly differentiated adenocarcinoma of the colon: subsite location and clinicopathologic features. Int J Colorectal Dis 2015; 30: 187-196.
21. Fiehn AM, Grauslund M, Glenthøj A, et al. Medullary carcinoma of the colon: can the undifferentiated be differentiated? Virchows Arch 2015; 466: 13-20.
22. Xiao H, Yoon YS, Hong SM, et al. Poorly differentiated colorectal cancers: correlation of microsatellite instability with clinicopathologic features and survival. Am J Clin Pathol 2013; 140: 341-347.

Address for correspondence

Małgorzata Kołos
Department of Pathomorphology in Warsaw
Central Clinical Hospital of the Ministry of the Interior
Wołoska 137
02-507 Warsaw, Poland
tel. +48 22 508 12 35
e-mail: malgosia.kolos@gmail.com